An EQCM Study of the Electropolymerization of Benzene in an Ionic Liquid and Ion Exchange Characteristics of the Resulting Polymer Film

O. Schneider, A. Bund,[†] A. Ispas,[†] N. Borissenko, S. Zein El Abedin,[‡] and F. Endres*

Institut für Metallurgie, Technische Universität Clausthal, Robert-Koch-Str. 42, D-38678 Clausthal-Zellerfeld, Germany

Received: November 8, 2004; In Final Form: February 9, 2005

The direct electropolymerization of benzene dissolved in the ionic liquid 1-hexyl-3-methylimidazolium tris(pentafluoroethyl)trifluorophosphate was studied at room temperature applying the electrochemical quartz-crystal microbalance technique. Analysis of the damping changes showed that the Sauerbrey equation could be applied for data evaluation. In the polymer, every third to fourth benzene ring carried a positive charge in the oxidized state. During electropolymerization, some ionic liquid was absorbed in the growing polymer. The redox behavior was characterized by wide peaks typical for conducting polymers. Charge neutrality of the polymer during redox cycling was maintained by anion and cation exchange with the ionic liquid. With increasing scan rate, cation exchange became more and more important.

1. Introduction

Electronically conductive polymers have been intensively studied since 1977.[1] Typical examples are polyacetylene, polypyrrole, polythiophene, poly(*p*-phenylene), polyaniline (Pani), and their derivates, but also many other heterocyclic or aromatic polymers.[2] Often, these polymers can be prepared by electrochemical oxidation from aqueous or nonaqueous electrolyte solutions containing the respective monomer. They are characterized by good electrical conductivity combined with low weight. The conductivity is based on the conjugated π-electron system and the formation of charge carriers such as polarons or bipolarons by doping. Doping is usually achieved by chemical or electrochemical oxidation of the polymer backbone, and in some cases (e.g., Pani), by exposure to acid. To maintain electroneutrality, doping is accompanied by the incorporation of counterions into the polymer matrix. The doped polymer therefore has a salt-like character. Dedoping (e.g., by electrochemical reduction) is accompanied by the expulsion of the counterions from the polymer or by additional incorporation of oppositely charged ions into the polymer. During electrochemical polymerization, the doped form of the polymer is usually obtained. The materials possess the potential for many applications, like antistatic coatings and composites, electromagnetic shielding, the production of integrated circuits, the controlled release of substances, ion-exchange membranes, electromechanic actuators, sensors, electrochromic materials, polymer LEDs, batteries, and corrosion protection.[3]

Poly(*p*-phenylene) (PPP) and its derivatives are interesting candidates for the construction of organic light-emitting diodes (OLED). It was shown by Leising et al. that with PPP blue light-emitting OLEDs can be made.[4−6] There is still a huge interest in PPP, and quite recently, it was shown that by single-molecule spectroscopy a universal picture of chromophores in π-conjugated polymers can be derived.[7] It is an attractive aim to make PPP by electrochemical means, as the properties of the deposit can be strongly influenced by the synthesis parameters. Furthermore, the doping degree of a conducting polymer can easily be adjusted by the proper choice of the electrode potential. In the past, the electropolymerization of benzene was only successful in solvents such as liquid SO_2, HF/SbF_5, or 18 M H_2SO_4, demanding experimental conditions.[8,9] Furthermore, there are a few studies on the electrodeposition of PPP in organic solvents.[10] Early studies on benzene electropolymerization in ionic liquids were based on $AlCl_3$-based solvents where chlorine evolution takes place at the positive potentials required to oxidize benzene.[11−14] Ionic liquids are a rather novel class of solvents that solely consist of cations and anions. They have extraordinary physical properties (e.g., they usually have negligible vapor pressures even at elevated temperatures) and furthermore, they can have electrochemical windows of up to 7 V.[12−18] As a consequence, they can easily be made water-free. On one hand, such reactive elements such as Si, Ge, Al, and others can be deposited in the cathodic regime, and on the other hand, such noble molecules as benzene and its derivatives can be oxidized. Recently, it was shown that benzene can easily be electropolymerized in the ionic liquid 1-hexyl-3-methylimidazolium tris(pentafluoroethyl)trifluorophosphate ([HMIm]FAP) to give polyphenylene.[19] In the present paper, the electropolymerization of benzene in [HMIm]FAP is investigated with the electrochemical quartz-crystal microbalance (EQCM).

The tracking of the resonance frequency of a quartz crystal is a well-established method to monitor small mass changes at the surface of the resonator (quartz-crystal microbalance, QCM).[20] In most applications (e.g., deposition rate monitoring in a vacuum), it is sufficient to drive the quartz crystal with an oscillator circuit and to measure the frequency with a frequency counter. However, if one deals with damping layers (such as viscoelastic or very rough layers), it is better to characterize the electrical behavior of the resonator around its resonance

* Corresponding author. Telephone: +49-(5323) 72 3141. Fax: +49-(5323) 72 2460. E-mail: frank.endres@tu-clausthal.de.

[†] Technische Universität Dresden, Institut für Physikalische Chemie und Elektrochemie, Mommsenstr. 13, D-01062 Dresden, Germany.

[‡] Permanent address: Electrochemistry and Corrosion Laboratory, National Research Center, Dokki, Cairo, Egypt.

10.1021/jp044892r CCC: $30.25
Published on Web 03/22/2005

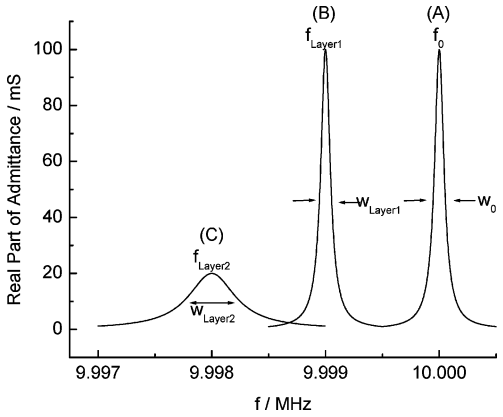

Figure 1. Resonance curve of a 10-MHz quartz crystal with different acoustic loads. (A) unloaded quartz, (B) quartz with smooth rigid layer, (C) quartz with damping layer.

frequency more completely. This can be done by measuring the real part of the electrical admittance of the quartz crystal with a network analyzer or an impedance bridge.[21−24] One obtains a resonance curve which can be described with a Lorentzian function (Figure 1). The center of the curve lies at the resonance frequency f; its full width at half-maximum (fwhm) w is proportional to the damping of the quartz crystal. If a smooth rigid layer is deposited on the quartz crystal (e.g., by vacuum evaporation) the resonance curve shifts to lower frequencies but does not change its form (Figure 1, transition from curve A to B). If the layer dampens the oscillation of the quartz crystal (e.g., a liquid), the resonance curve shifts to lower frequencies and at the same time broadens (Figure 1, transition from curve A to C).

From the shift of the curve, a complex frequency shift Δf^* can be defined (eq 1, $i^2 = -1$) whose real part is the shift of the maximum of the resonance curve and whose imaginary part contains the change of the fwhm.[25,26]

$$\Delta f^* = (f_{\text{layer}} - f_0) + i/2(w_{\text{layer}} - w_0) \tag{1}$$

The mechanical behavior of the layer can be described by its mechanical impedance Z_M^*, which is directly proportional to Δf^* (eq 2).[26]

$$Z_M^* = (-i\pi Z_Q/f_0)\Delta f^* \tag{2}$$

with Z_Q the mechanical impedance of the quartz crystal (8.849×10^6 kg m^{-2} s^{-1}), $i^2 = -1$, and f_0 the fundamental resonance frequency of the unloaded quartz.

In the simplest case, a smooth rigid layer with density ρ and thickness L, $Z_M^* = i2\pi f\rho L$, and the well-established Sauerbrey equation results (eq 3) [27]

$$\Delta f = -\frac{2f_0^2}{Z_Q}\rho L = -\frac{2f_0^2}{Z_Q}\frac{\Delta m}{A} \tag{3}$$

where $\Delta m/A$ is the change of the areal mass density.

Note that in this case the frequency shift is a purely real quantity (i.e., no damping change occurs). This is a consequence of the smoothness and rigidity of the layer. However, electrochemically prepared layers often have a certain surface roughness which strongly depends on the preparation conditions. The damping of the quartz gives a first indication if the Sauerbrey equation can be applied.[28−30]

The EQCM technique has been applied extensively in the literature to study synthesis and ion-exchange properties of conducting polymers in aqueous and conventional organic electrolyte solutions,[30−41] partly in combination with other techniques.[42−45] In this work, we applied the EQCM technique to study the electropolymerization of benzene in an ionic liquid. Furthermore, the polymerization reaction as well as the ion-exchange characteristics of the resulting film in the ionic liquid were studied.

2. Experimental Section

The quartzes were blank, polished 10-MHz AT cut crystals provided by KVG (Neckarbischofsheim, Germany). Pulsed-laser deposition (chamber pressure = $(3-6) \times 10^{-6}$ mbar; pulse energy $\approx$ 250 mJ) was used to deposit a titanium adhesion layer (10 pulses/s, ca. 15−20 nm) and Pt electrodes (40 pulses/s, ca. 150 nm). The piezoelectric active area was 0.24 cm^2; the electrochemically active area was 0.277 cm^2. The quartz was placed at the bottom of a cylindrical poly(tetrafluorethylene) (PTFE) cell (home-built). The electrochemical cell and the quartz were cleaned in a mixture of concentrated sulfuric acid/30% aqueous hydrogen peroxide and subsequently refluxed in double distilled water. In the experiments, the quartz was held between two O-ring gaskets. On the ionic liquid side, it is essential to use a perfluoroelastomer such as Kalrez (Dupont Dow Elastomers L.L.C., Newark, Delaware, U.S.A.). Otherwise, swelling of the gasket could lead to considerable signal drifts. The cell with the quartz was transferred to an Ar-purged glovebox (Vacuum Atmospheres OMNILAB), in which all solutions were prepared and all electrochemical experiments were conducted. The potential of the Pt electrode facing the ionic liquid was controlled with a PAR Versastat II potentiostat; the other electrode faced the inert-gas atmosphere of the glovebox. The potentials were measured versus a Pt quasi-reference electrode which gave a sufficiently stable electrode potential for the time frame of the experiments. The counter electrode was Pt foil.

Electrochemical polymerization was performed in 10 mL of a solution of 0.2 M benzene in the room-temperature ionic liquid (IL) [HMIm]FAP. [HMIm]FAP (Merck, high purity) was dried prior to use at 110−120 °C at a pressure of 0.001 mbar overnight. Ion chromatography did not show any inorganic impurities. The molar mass of the IL cation $[HMIm]^+$ is 167 g mol^{-1}, and the mass of the anion is 445 g mol^{-1}. It has been shown elsewhere that in this IL the ferrocene/ferricenium redox couple showed a reversible wave with $E_{1/2} = 0.55 \pm 0.05$ V versus a Pt quasi-reference electrode.[19] Polymerization was accomplished by cycling the potential between 0 and 2.2 V versus Pt at a sweep rate of 10 mV/s. Characterization of the resulting polymer film was done after exchange of the solution for a benzene-free one. Cyclic voltammograms were recorded in the same potential range used for polymerization at sweep rates of 10, 20, 40, 50, and 100 mV s^{-1}.

The electrical admittance curve of the quartz was measured parallel to the electrochemical experiments with a network analyzer (Agilent E5100A) and transferred to a PC-compatible computer via a general purpose interface bus (GPIB) interface. To reduce the data (each admittance spectrum consisted of 801 data points), the real part of the admittance curve was fit with a Lorentzian. Approximately every 500 ms, one data set could be acquired, consisting of the resonance frequency f, the fwhm w, and the current, potential, and charge (for details, see ref 46). Mass data were calculated according to eq 3, on the basis of the resonance frequencies and the well-known Z_Q for the quartz crystal. The first resonance frequency measured in each

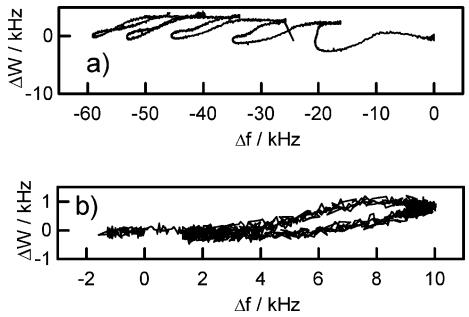

Figure 2. Change in damping Δw and resonance frequency Δf during electropolymerization (a, 0−2.2 V, 10 mV s^{-1}) and during cyclic voltammetry of polymer in benzene-free IL (b, 0−2.2 V, 20 mV s^{-1}).

experiment was taken as the fundamental frequency f_0. Frequency changes Δf were then calculated for each data set as $f - f_0$.

Scanning electron microscopy (SEM) investigations were performed with a Zeiss DSM 982 Gemini microscope (Carl Zeiss, Germany) at an acceleration voltage of 4 kV.

3. Results

3.1. Validation of the Sauerbrey Approach. Upon filling the QCM cell with the ionic liquid, the resonance frequency of the quartz decreased by about 24 kHz, and the damping increased to 49 kHz, and thus, the presence of the IL caused a complex frequency shift of $\Delta f^* = (-24 + i24.5)$ kHz (eq 1). These values are typical for the quartz resonators used in this study.

Figure 2 shows the change in damping as a function of the change in the resonance frequency during the polymerization (Figure 2a) and, after solution exchange, during characterization at a sweep rate of 20 mV/s (Figure 2b). Note that the same scale is used for *x* and *y* axes in the plots. It can be clearly seen that the changes in the damping are much smaller than the changes in the resonance frequency. As will be discussed later, this justifies the application of Sauerbrey's equation, eq 3, to convert the measured resonance frequencies to mass changes. All mass data shown in the following sections have been calculated that way. Mass changes are due to the formation of a polymer on the electrode and to the incorporation (or expulsion) of ions from the IL into (out of) the polymer.

3.2. Electrochemical Polymerization. Figure 3 shows the cyclic voltammograms of electrochemical polymerization as well as the first derivation of the mass change with respect to time. The latter is the direct mass analogue of electrical current and has been used in the literature.[37,39] In the first anodic cycle, at potentials below 1.79 V, current densities were on the order of microamperes per square centimeter, and the mass load of the resonator was constant. Above that potential, a steep increase in the current typical for an electropolymerization reaction could be observed. From the beginning, this current was accompanied by an irreversible mass increase. During the subsequent cathodic sweep, a shoulder and a cathodic wave could be observed in the voltammogram, and in the second anodic sweep, a broad oxidation peak appeared. The cathodic wave was characterized by a decrease of the mass on the electrode and the anodic peak by a mass increase. Cathodic and anodic peak currents increased from cycle to cycle, as well as the mass changes associated with it. The position of the anodic peak shifted to higher potentials from cycle to cycle, whereas the cathodic peak potential remained almost constant. During the experiment, a dark film formed on the electrode.

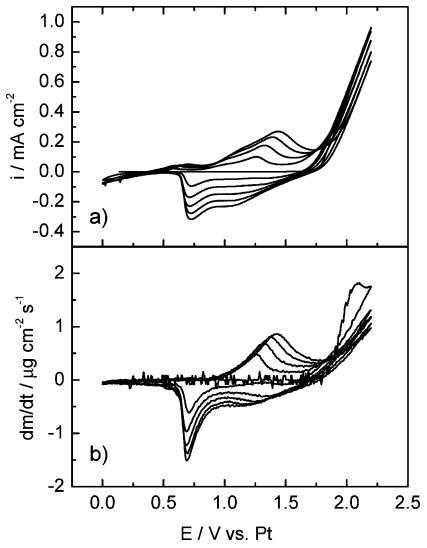

Figure 3. Voltammograms (a) and differential mass change (b) during potential cycling between 0 and 2.2 V vs Pt in a solution of 0.2 M benzene in [HMIm]FAP. Scan rate: 10 mV s^{-1}.

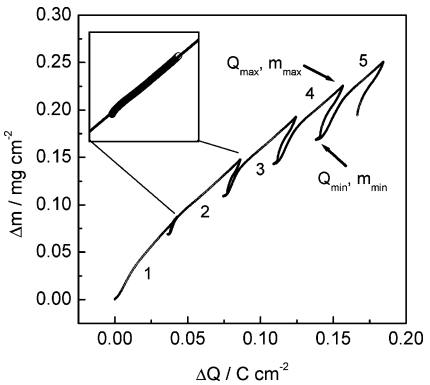

Figure 4. Mass and charge flux during the electropolymerization experiment shown in Figure 3 for all five cycles. The cycle number is indicated in the figure. In each cycle, charge and mass of the polymer showed maxima after the end of the polymerization (Q_{max}, m_{max}) and decreased during film reduction to minima (Q_{min}, m_{min}). In the electropolymerization region, mass scaled linearly with charge, and the slope d*m*/d*Q* was determined by linear regression, as indicated for cycle 2 in the insert. The fit line has been extended for improved visibility.

Figure 4 relates the charge and mass changes in the experiment. The (mostly irreversible) increase in charge due to electropolymerization was accompanied by a (mostly irreversible) increase in the mass of the film on the electrode, whereas the (reversible) decrease of the charge caused by the reduction process coincided with a (reversible) mass decrease. Overall, there was a net anodic charge and a net mass increase, as expected for an anodic electrodeposition process.

On the basis of the data in Figure 4, it is possible to determine the ratio of reversible and irreversible charge (r_q) and mass flux (r_m) according to

$$r_q = \frac{Q_{rev}}{Q_{irr}} = \frac{Q_{max} - Q_{min}}{Q_{min}} \quad (4)$$

$$r_m = \frac{m_{rev}}{m_{irr}} = \frac{m_{max} - m_{min}}{m_{min}} \quad (5)$$

The results of the calculations are given in Table 1, along with the increase in irreversible charge (ΔQ_{irr}, calculated as the increase in Q_{min} from one cycle to the next one) and mass (Δm_{irr},

TABLE 1: Charge and Mass Changes during Electropolymerization of Benzene[a]

cycle	ΔQ_{irr}	Δm_{irr}	r_q	r_m
1	0.0363	0.0687	0.176	0.270
2	0.0381	0.0403	0.159	0.544
3	0.0345	0.0339	0.142	0.349
4	0.0292	0.0257	0.134	0.339

[a] Irreversible charge (ΔQ_{irr}) and mass change (Δm_{irr}) per cycle (calculated from the increases in Q_{min} and m_{min} from cycle to cycle) and ratio of reversible and irreversible charge (r_q) and mass flux (r_m) for the electropolymerization experiment shown in Figure 3. [ΔQ_{irr}] = C cm^{-2}; [Δm_{irr}] = mg cm^{-2}.

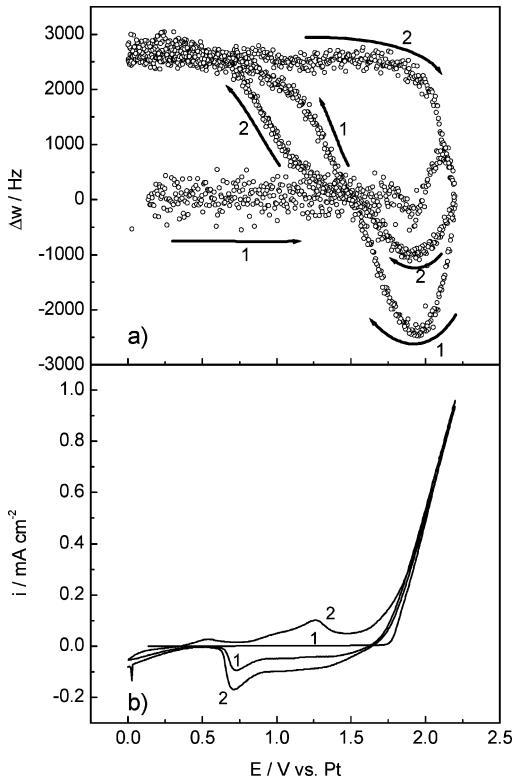

Figure 5. Change in the damping of the resonator during the first two cycles. (a) damping changes, (b) corresponding voltammogram. The numbers indicate the voltammetric cycle and arrows the sweep direction.

calculated from the corresponding increase in m_{min}) in each cycle. Note that the irreversible charge in the second cycle was larger than in the first one, but decreased thereafter from cycle to cycle. The irreversible mass change decreased right from the beginning. The largest mass increase was observed in the first cycle. Reversible charge and mass flux increased from cycle to cycle.

For the data analysis of EQCM measurements, the mass−charge ratio is of importance.[29,38,41,47] In the range of polymerization, the $\Delta m/\Delta Q$ plot was almost linear in each cycle. Therefore, $\Delta m/\Delta Q$ was determined from the slope of the line fits in these regions (cf. insert in Figure 4). In the very beginning of the polymerization, the slope was 0.001 67 ± 0.000 02 g/C. Later in the first cycle, a transition occurred, and in the end, the slope was 0.001 729 ± 0.000 003 g/C. In subsequent cycles, the average slope was found to be 0.001 35 ± 0.000 015 g/C.

The formation of the film on the electrode was accompanied not only by a change in the resonance frequency of the resonator but also by a change in the damping. This is shown for the first two cycles of electropolymerization in Figure 5: After an initial increase of the damping during the first polymer formation, a decrease of the damping to values lower than for the bare

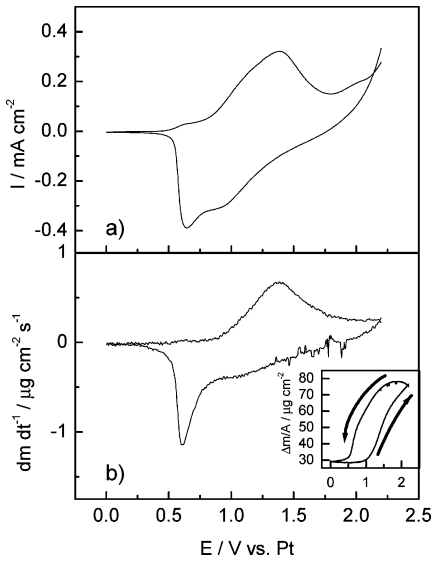

Figure 6. Cyclic voltammogram of the polymer film in pure IL at a scan rate of 10 mV/s (a) and the corresponding mass derivative (b). The insert shows the total mass change in the cycle as a function of the electrode potential. Arrows indicate sweep direction.

electrode was observed. Reduction of the polymer then caused a tremendous increase in the damping by almost 5 kHz. In subsequent cycles, polymerization always caused a damping decrease and film reduction caused a damping increase.

3.3. Cyclic Voltammetry of Polyphenylene in the Pure Ionic Liquid. The general shape of cyclic voltammograms and the concurrent mass changes are shown in Figure 6 for a scan rate of 10 mV/s. As already seen in the synthesis voltammograms (Figures 3 and 5), the peaks were rather broad and widely separated. Two regions could be identified in the cathodic sweeps: A region where an increasing cathodic current was observed without expressing a clear peak, and a sharp peak at lower potentials. This is more clearly visible in the corresponding dm/dt plot. In the anodic direction, after a very small shoulder, only one large peak was observed that appeared to be asymmetric. With increasing scan rates, anodic and cathodic peak potentials both shifted to more extreme values, and the peaks became wider. The color of the polymer film changed during the potential sweep: It was brighter in the reduced state, and it became deeply black in the oxidized state.

The scan-rate dependence of the peak potentials and currents was the same as found in an earlier study.[19] Anodic and cathodic currents scaled linearly with the square root of the scan rate. The intercept of the linear fits was not zero, though. Cathodic peak currents were larger than anodic peak currents. The peak values of dm/dt increased with the scan rate as well.

The insert in Figure 6 shows the corresponding mass−potential diagram. The potentials associated with the maxima and minima in the mass curves coincided with those of zero crossing of currents in the cathodic and anodic sweep, respectively. At higher scan rates, the mass minimum in the anodic sweep shifted to potentials positive of zero crossing.

With increasing scan rate, the damping shifted to larger values. The difference between the damping of the oxidized polymer and the reduced polymer increased, and the difference between anodic and cathodic sweep (i.e., the hysteresis) became larger. This is shown in Figure 7 for scan rates of 10 and 40 mV/s. A similar, even more pronounced hysteresis was obtained for the frequency (and thus mass) data.

For a potential sweep at 20 mV/s between 0 and 2.2 V, the integral changes in mass and charge during oxidation and

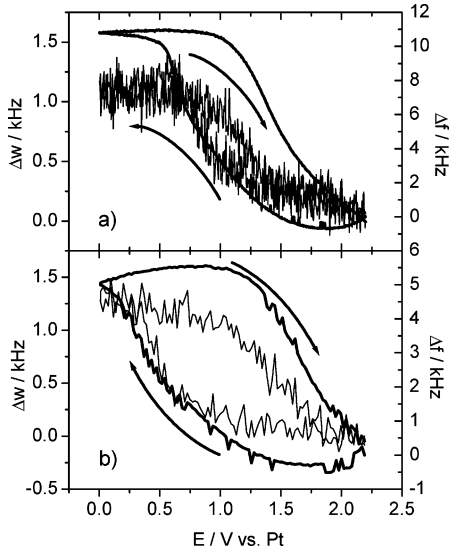

Figure 7. Change in damping (thin line) and frequency (bold line) during cyclic voltammetry at 10 (a) and 40 mV/s (b) between 0 and 2.2 V vs Pt in benzene-free IL. Arrows indicate sweep direction.

TABLE 2: Typical Mass and Charge Data Measured during Cyclic Voltammetry of Polyphenylene in Benzene-Free Ionic Liquid[a]

cycle	Δm (an)	ΔQ (an)	$\Delta m/\Delta Q$ (an)	Δm (ca)	ΔQ (ca)	$\Delta m/\Delta Q$ (ca)
1				−48.2	−25.6	0.00188
2	36.5	25.5	0.00143	−36.3	−22.2	0.00163
3	36.2	25.4	0.00143	−35.4	−22.1	0.00160
4	34.8	25.2	0.00138	−34.2	−22.1	0.00154

[a] Changes in mass (Δm) and charge (ΔQ) during oxidation (an) and reduction (ca) of the polymer, measured at 20 mV/s between 0 and 2.2 V vs Pt. [Δm] = μg cm^{-2}; [ΔQ] = mC cm^{-2}; [$\Delta m/\Delta Q$] = g/C.

reduction are given for all cycles in Table 2. Such data can be used to investigate the ion-exchange processes within the polymer.

Both mass and charge flux decreased from cycle to cycle. Anodic charges were always larger than the cathodic ones, causing a drift in the signal. The drift in the mass curve was smaller.

Figure 8 shows for a scan rate of 20 mV/s the typical mass−charge plots. The anodic scan shows a simple sigmoidal-type curve (Figure 8a). The slope is always positive. Instead of using integral mass and charge data, differentiation of the mass signal for the charge allows a more detailed analysis of electrochemical processes during the polymer redox reaction and especially allows the determination of potential dependent properties. Differential data are given in the inserts in Figure 8. For the oxidation cycle, dm/dQ increased, reached a maximum, and decreased thereafter. All values at positive currents were positive.

For the cathodic scan (Figure 8b), the plots look different. Several regions of the $\Delta m-\Delta Q$ curve are marked. At high potentials (region 1), there was still some oxidation going on causing an increase in charge and mass. The current crossed zero, and film reduction set in (region 2). From then on, the slope of the curve changed only gradually (regions 3−7). At very low potentials, though, the slope became much more negative (region 9). The insert compares the dm/dQ values as determined by linear regression in the regions marked (which eliminates artifacts from low current noise) to the ones obtained from direct differentiation of the curve in Figure 8b. This demonstrates that the very high scatter of data to lower and

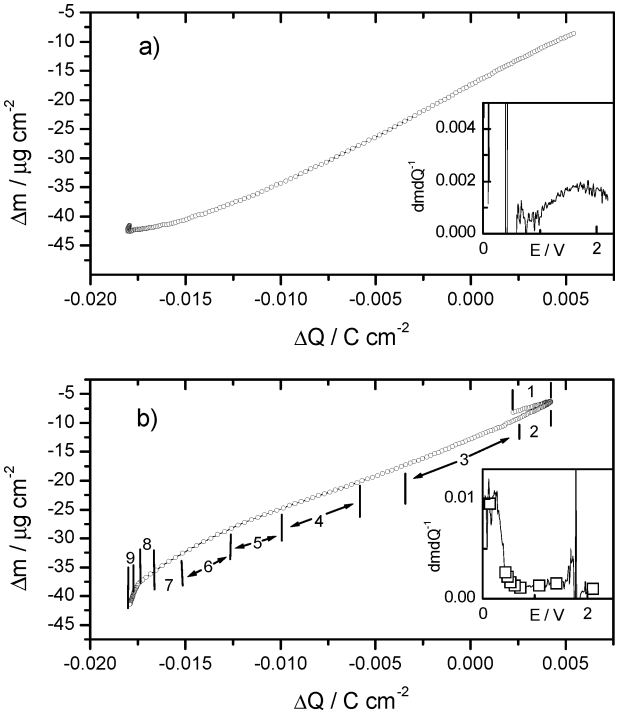

Figure 8. Mass−charge curves for the second full cycle between 0.0 and 2.2 V at 20 mV/s. (a) Anodic sweep: insert shows dm/dQ. (b) Cathodic sweep: several regions are labeled. Within these regions, linear regression was performed to obtain average values for dm/dQ. Those average numbers are given in the insert as open squares, together with the result of the direct derivation of Δm for ΔQ (line). [dm/dQ] = g/C.

higher numbers between regions 1 and 2 is caused by the zero crossing of the current (dQ = 0, and thus, dm/dQ not well-defined). However, at all other potentials, there was good agreement between the values determined by both methods, especially at low potentials (region 9) also. With decreasing potential and thus increasing reduction of the film, dm/dQ decreased slightly until a minimum had been reached. At the approach of complete reduction, dm/dQ strongly increased. With an increase of scan rate, there was no general change in the shape of Δm versus ΔQ plots. In the anodic sweeps, the potential of zero crossing shifted to higher potentials, and a small region of negative dm/dQ was seen. In the cathodic sweeps, the increase in dm/dQ at low potentials became less pronounced. The range of mass and charge change during the redox process decreased with increasing scan rate.

3.4. Scanning Electron Microscopy. Figure 9 shows two SEM images of the films obtained on the quartz crystals after polymerization. They show a rather rough, porous polymer structure. Some fiberlike polymer strands can be seen, which seem to be a major component of the polymer film.

4. Discussion

4.1. Changes in the Damping of the Quartz Resonators. The total half-bandwidth of the resonance curve was more than 50 kHz. The major contributions to this high damping are the large viscosity, η, and density, ρ, of the ionic liquid [HMIm]-FAP. The values are η = 0.115 Pa s and ρ = 1.56 g cm^{-3}, which is more than 100× the viscosity of water.[48] The influence of the viscosity−density product of the solution on the resonance behavior has been discussed extensively in the literature.[49−51] For a Newtonian liquid, $\Delta f = \Delta w/2 = f_0^{3/2}(\eta\rho/\pi)^{1/2}/Z_Q$. Thus, the $\eta\rho$ value of [HMIm]FAP gives $\Delta f \approx 28\,000$ s^{-1} and also explains the high damping of the quartz.

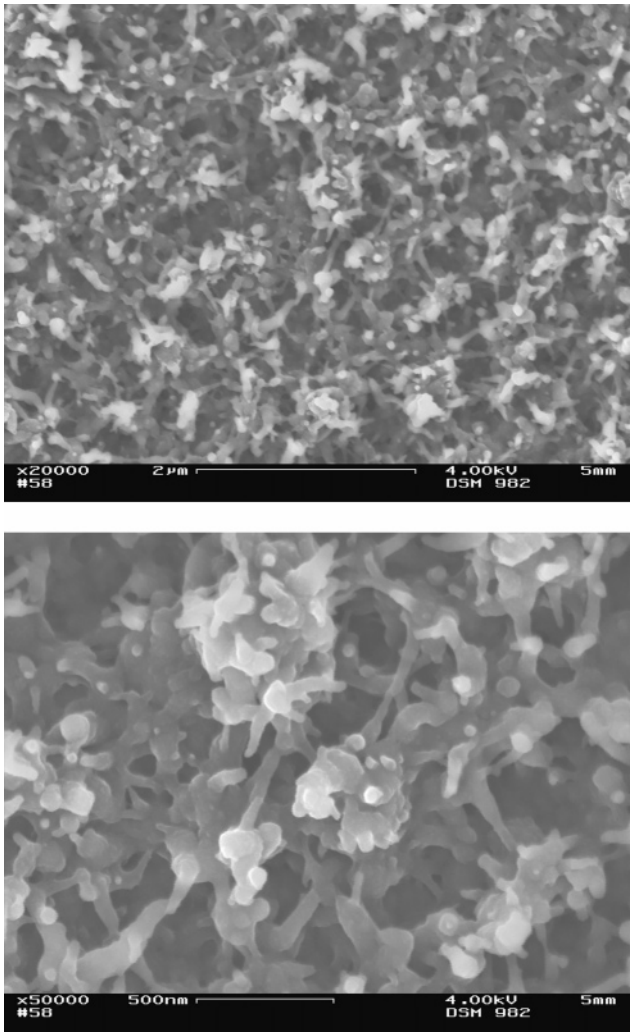

Figure 9. SEM images recorded from the polymer produced by electropolymerization of benzene at magnifications of 20 000× and 50 000×.

The increase in damping during the polymer film reduction can be related to a change in surface roughness due to the structural changes, when the salt-like oxidized form of the polymer is reduced to a presumably more hydrophobic form. This transformation could be accompanied by a volume change. However, at this point, there are no data about the structure of this polymer in oxidized or reduced form. The large difference in anodic and cathodic peak potentials (Figure 3 and Figure 6) even at low scan rates can be indicative of structural changes coupled to the change in oxidation state, though. This has been shown for other conducting polymers.[52] Another possibility to explain the damping changes is a change of the viscoelastic properties of the polymer itself upon its conversion from the more rigid oxidized form to the less rigid reduced form. Viscoeleastic properties of coatings have a strong influence on the damping of piezoelectric resonators.[28,30,53−55] For polypyrrole, an increase in the damping upon reduction has been reported and interpreted by volume changes.[41]

Problems concerning the applicability of the Sauerbrey equation can arise from several sources. One of them is the presence of viscoelastic, nonrigid, or rough films on the resonator, like thick layers of polymer.[28,30,53,56,58] The Sauerbrey equation can only be applied without correction to situations where the films are acoustically thin.[14,40,58] This is the case when their thickness, multiplied by the density, is only about 2% of the resonators' thickness, multiplied by its density. For the polymer in this study, a thickness of about 2.5 μm can be determined from the mass increase during polymerization (Figure 4), if one assumes a density of about 1 g cm^{-3} (a typical value for conducting polymers[10]). Therefore, the acoustical thickness is only about 0.6% of that of the resonator ($d = 167$ μm; $\rho = 2.648$ g cm^{-3}),[59] and rigid film can be assumed. This is also supported by the good linearity observed in the $m-Q$ plot (Figure 4), as has been shown for other polymers.[10,38]

TABLE 3: Degree of Doping x and Amount of Ionic Liquid Absorbed in Polymer Film[a]

	1	2	3	4
cycle	x (eq 6)	dm/dQ (Figure 4)	x (eq 7)	y_{IL} (eq 8)
1	0.352	0.001729	0.926	0.261
2	0.318	0.001363	0.597	0.143
3	0.284	0.001364	0.597	0.160
4	0.268	0.001335	0.574	0.158
5		0.001355	0.590	

[a] x = maximum degree of oxidation of conducting polymer; y_{IL}= amount of ionic liquid incorporated per mole of benzene, calculated using x in column 1. [dm/dQ] = g/C.

Another problem in applying the Sauerbrey equation can arise from surface roughness and the change of the coupling of the solution to the quartz.[29,60,61] In this work, we had the advantage of measuring the damping changes in the experiments and thus to assess directly the applicability of Sauerbreys equation from Δw versus Δf plots. Figure 2 clearly shows that during the preparation and characterization the frequency changes were at least 1 order of magnitude larger than the damping changes, or in other words, the real part of Δf^* is much larger than the imaginary part. It is generally accepted in the literature that under these conditions the real part of Δf^* can be converted to a mass change using eq 3.[22,28,57,62,63]

4.2. Maximum Degree of Doping. As for other polymers, the charge needed for the formation of the oxidized polymer can be related to the (irreversible) charge needed to build the polymer backbone ($2F$ per mole of benzene; $F = 96\,487$ C/mol) and the (reversible) charge needed to oxidize the polymer, until it reaches the degree of oxidation x ($x \cdot F$ per mole of benzene). The latter charge should be identical to the cathodic charge measured during the cathodic sweep under the assumption that the entire polymer film is reduced in the cathodic sweeps. Then, it is possible to calculate x from the electrochemical charge data given in Figure 4 and Table 1

$$x = 2r_q \tag{6}$$

The results for the first four synthesis cycles are displayed in column 1 of Table 3. They represent reasonable values for the degree of doping x of a conducting polymer. In the fully oxidized state, every third to fourth benzene ring carries a positive charge. With increasing thickness of the polymer, the reduction reaction apparently no longer involves the entire polymer, leading to lower apparent degrees of doping. Plotting $Q_{max} - Q_{min}$ versus Q_{min} (cf. Figure 4) and performing a linear regression gives the smaller number of $x = 0.24$.

Alternatively, x can be calculated from the slope of the linear regions in the $\Delta m-\Delta Q$ plot (Figure 4). The mass change is due to the effective mass of the benzene rings in the polymer (76 g/mol of benzene) and the amount of counteranions incorporated into the polymer to compensate for the positive charges within the polymer (445 g × x per mole of

benzene). Therefore, one can write

$$\frac{dm}{dQ} = \frac{M_{C_6H_4} + x \cdot M_{anion}}{(2 + x) \cdot F}$$

$$x = \frac{M_{C_6H_4} - 2F\left(\frac{dm}{dQ}\right)}{F\left(\frac{dm}{dQ}\right) - M_{anion}} \quad (7)$$

Table 3 gives the slopes dm/dQ from Figure 4 (column 2) and x calculated from eq 7 (column 3). The degrees of doping thus obtained are twice as large or even larger compared to those from coulometric data, and are no longer reasonable. The increase in mass measured is therefore larger than expected from the charge measured and from the molar masses of benzene and the FAP anion. A possible explanation is that a certain amount of ionic liquid has been absorbed into the film during polymerization. To calculate the number y_{IL} of moles of ionic liquid absorbed per mole of benzene in the film, eq 7 has to be modified

$$\frac{dm}{dQ} = \frac{M_{C_6H_4} + x \cdot M_{anion} + y_{IL} \cdot M_{IL}}{(2 + x) \cdot F}$$

$$y_{IL} = \frac{(2 + x) \cdot F \cdot \left(\frac{dm}{dQ}\right) - M_{C_6H_4} - x \cdot M_{anion}}{M_{IL}} \quad (8)$$

Using x from electrochemical data (Table 3, column 1), one can calculate y_{IL}. This number is displayed in column 4 and corresponds to about one unit of ionic liquid (one anion + one cation) every fifth−seventh benzene ring. Similar results for y_{IL} are obtained from the values of Δm_{irr} and ΔQ_{irr} for cycles 2−4 shown in Table 1. This shows that even in the reduced state a significant amount of ionic liquid is retained in the polymer.

There is another aspect that requires consideration: In electropolymerization reactions, a certain amount of material can be lost in the form of oligomers soluble in the solvent. This has been shown to play a crucial role in the synthesis of poly(*p*-phenylene) from the polymerization of oligo(*p*-phenylene) in acetonitrile.[10] Therefore, the current efficiency η_i might be smaller than 1. Equations 6 and 8 can be modified to incorporate the current efficiency. In eq 6, the right-hand side needs to be divided by η_i, and in eq 8, Faraday's constant needs to be divided by η_i. A current efficiency of less than 1 would mean that the degree of doping and the amount of ionic liquid in the polymer actually were larger than the values shown in Table 3. At a current efficiency of 90% (80%) for the fourth cycle, an x value of 0.298 (0.335) instead of 0.268 and a y_{IL} value of 0.197 (0.247) instead of 0.158 would be obtained. Therefore, the values from Table 3 are lower limits for the degree of doping and the incorporation of ionic liquid.

4.3. Anion and Cation Exchange during Reduction and Reoxidation of the Polymer Backbone. Charge compensation during reduction of the positively charged polymer backbone can be accomplished by expelling counteranions into the electrolyte or by incorporating cations into the polymer, forming a nominally neutral electrolyte. The opposite processes are possible during the oxidation reaction. Cations can only be expelled during oxidation of a conducting polymer as long as some mobile cations are present in the film, and they only can be incorporated during reduction if space is available.[38] During electropolymerization itself, charge compensation requires the incorporation of anions. In common electrolytes, a solvent and a neutral salt can be incorporated or expelled from the polymer film in addition to the ion-exchange processes, which complicates matter significantly. In fact, under these circumstances, it is no longer possible from EQCM to separate anion- and cation-exchange processes accurately without additional experimental data (like the probe beam deflection method).[43−45] In ionic liquids, however, the electrolyte itself is the solvent. Therefore, only anions and cations can be involved in the redox reaction of the polymer. Thus, it should be possible to split the total mass flux in function of the electrode potential into the (molar) contributions from the cations ($z_c(E)$) and anions ($z_a(E)$) based on EQCM data alone, using procedures similar to those applied for polymers in aqueous solutions.[36,37]

The following equations are used for the calculation of z_a and z_c (for derivation, see Appendix):

$$z_a(E) = \frac{\left(\frac{dm}{dQ}\right)_E \cdot F + M_{cation}}{M_{IL}}$$

$$z_a(E) + z_c(E) = 1 \quad (9)$$

However, it is still possible that IL formed within the polymer by cation ingress or included during polymerization is expelled at a later stage of reduction (e.g., by structural changes of the polymer backbone). This corresponds to salt transfer in aqueous electrolytes. This additional mass change is unrelated to the current measured at that time. In the data analysis, this process will reflect in an apparently increased contribution of anions to the redox process. Equation 9 then no longer gives correct exchange coefficients $z_a(E)$ and $z_c(E)$ related to the electrical current. Thus, $z_a(E)$ and $z_c(E)$ should be termed apparent exchange coefficients, because they may contain the contribution from the IL expelled. Under most circumstances, it is not necessary to distinguish between real and apparent exchange coefficients, because insertion of a cation accompanied by the expulsion of one unit of ionic liquid is formally the same as the expulsion of an anion. This situation has been discussed (for polypyrrole) in detail in the "cube" model for aqueous electrolytes in the context of salt transfer.[38] The additional contribution from IL expulsion, however, can cause $z_a(E)$ to become larger than 1 and the corresponding $z_c(E)$ to become negative. A complete mathematical treatment is given in the Appendix.

Figure 10 shows the results obtained from eq 9 for the second voltammetric cycle between 0 and 2.2 V at a scan rate of 20 mV/s in benzene-free solution. The apparent anion exchange coefficients are calculated from dm/dQ data corresponding to those shown in the inserts in Figure 8. In the cathodic half-cycle, the z_a data are omitted in the range where the current changes from anodic to cathodic (and thus, dQ becomes 0). From current data, it can be seen that a large portion of reduction occurs at potentials above the cathodic peak potential. Especially during the reduction in this potential range, there is a significant contribution of cation ingress. In the region where the cathodic peak is observed, anion exchange becomes the dominant process. However, values of more than 100% are observed when the polymer approaches complete reduction. This indicates that, indeed, some additional ionic liquid is expelled. This is similar to the reduction of polypyrrole in aqueous solutions and of PPP in acetonitrile, where the transfer of neutral species (salt, solvent) into solution has been observed especially for strong reduction.[10,38,43] Similar to cation ingress during cathodic reduction,

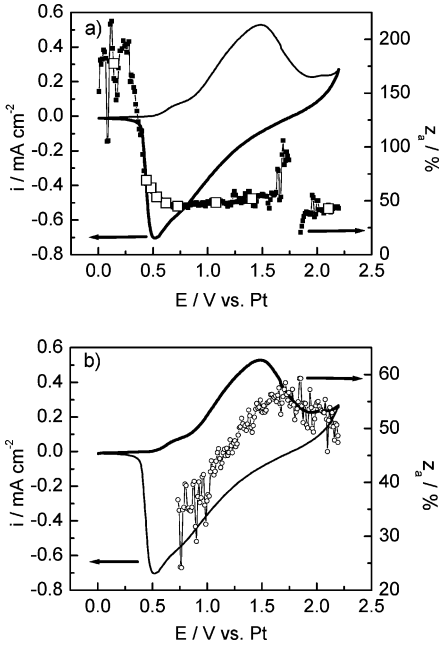

Figure 10. (a) Apparent anion exchange coefficients z_a (filled squares, calculated directly from eq 9; open squares, calculated from discrete values for d*m*/d*Q* obtained by linear regression, cf. Figure 8) during a cathodic sweep of the polymer film immersed in [HMIm]FAP. (b) Apparent anion-exchange coefficients during subsequent anodic sweep (open circles). Lines: Corresponding cyclic voltammogram. Scan rate: 20 mV/s.

TABLE 4: Average Anion Exchange Coefficients at 20 mV/s[a]

cycle	$\bar{z}_a$, cathodic	$\bar{z}_a$, anodic
1	0.55	0.51
2	0.52	0.50
3	0.52	0.50
4	0.51	0.48

[a] The data were calculated separately for each anodic and cathodic sweep during the cyclovoltammetric experiment, applying eq 10.

cation egress plays an important role in anodic reoxidation of the polymer films.

Despite the restrictions discussed already, and opposite to aqueous and organic solvents, the total (average) flux of anions and cations out of the film across the entire potential range can be calculated from EQCM data alone. Therefore, an average value for z_a, $\bar{z}_a$, can be defined by eq 10

$$\bar{z}_a = \frac{\int_{E_1}^{E_2} z_a(E)\cdot I(E)\,\mathrm{d}E}{\int_{E_1}^{E_2} I(E)\,\mathrm{d}E} \qquad (10)$$

For this calculation, a meaningful potential range is selected where the currents are purely anodic or cathodic, where no side reactions take place, and where the noise in d*m*/d*Q* does not disturb. The results for the cyclic voltammetry at 20 mV/s are given in Table 4. The values found for anodic and cathodic sweeps are very similar and do not strongly change with time. Anions and cations contribute almost equally (on a molar basis) to the charge balance during the polymer reduction and oxidation. It is also possible to calculate average anion exchange coefficients from the integral charge and mass changes given in Table 2. Averaged across all cycles, one obtains a $\bar{z}_a$ value of 0.53 for the cathodic sweeps and 0.50 for the anodic ones. The results from both methods are therefore virtually identical.

TABLE 5: Scan Rate Dependence of Average Anion Exchange Coefficients, Calculated by eq 10

v/mV s^{-1}	$\bar{z}_a$ (anod)	$\bar{z}_a$ (cath)
10	0.56	0.60
20	0.50	0.53
40	0.44	0.46
50	0.43	0.43
100	0.39	0.38

This is also true for other scan rates. Table 5 gives the average anion exchange coefficients for different scan rates. Apparently, anion exchange becomes more and more unfavorable at higher scan rates.

From the $z_a(E)$ data, one can calculate partial voltammograms reflecting anion and cation exchange

$$i_a(E) = z_a(E)\cdot i(E)$$

$$i_c(E) = i(E) - i_a(E) \qquad (11)$$

These are shown for 10 and 50 mV/s in Figure 11. It is obvious that, at low scan rates, anion exchange is very important, especially in the region where the narrow cathodic peak shows up in the voltammogram. Outside the cathodic peak region, anion and cation exchange contribute almost equally to the overall cathodic current. Also in the anodic peak region, anion exchange dominates. At elevated scan rates, cation exchange becomes the dominant process over the entire potential range, and the shapes of the partial- or ion-specific voltammograms become very similar. This can be explained by the large size of the anion. Whereas at slow scan rates, there is enough time for

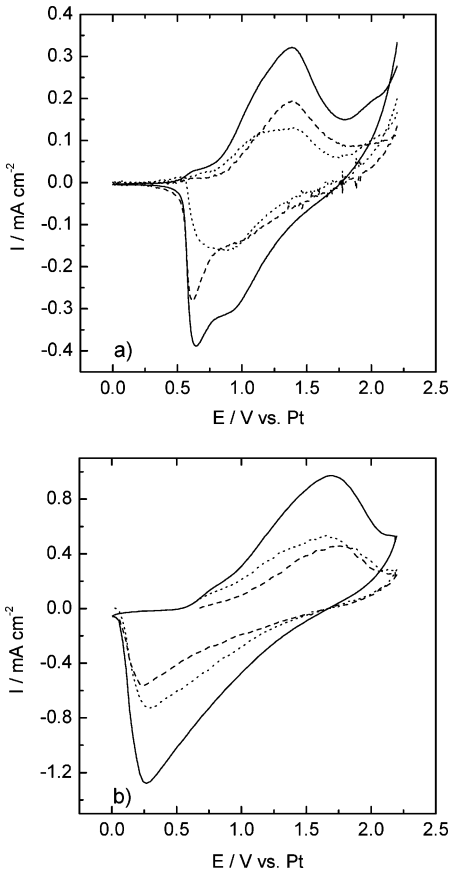

Figure 11. Cyclic voltammograms (solid lines) and partial currents due to anion exchange (dashed lines) and cation exchange (dotted lines) at 10 mV/s (a) and 50 mV/s (b).

the anion to be removed or inserted into the polymer film, this becomes increasingly difficult as the scan rate becomes larger.

Similar trends have been seen in cyclic voltammetry of polypyrrole (PPy) in sodium tosylate solutions, which showed on a mass basis a crossover from a net anion to a net cation exchange with an increase in scan rate, and even within single sweeps as a function of potential.[38] For our polymer (with the exception of a small potential range during oxidation at high scan rates) anion exchange still dominated the mass response at higher scan rates because of its large molar mass. This is why at all scan rates dm/dQ remains positive at (almost) all potentials. At low scan rates, kinetics of anion and cation exchange seem to be behave very differently, especially with respect to the potential dependence. At higher scan rates, when only a part of the polymer is reduced, this difference cancels out, and anionic and cationic currents look very similar in cyclic voltammograms.

5. Conclusions

Polyphenylene was deposited onto the quartz resonator of an electrochemical quartz-crystal microbalance by direct polymerization of benzene dissolved in the ionic liquid 1-hexyl-3-methylimidazolium tris(pentafluoroethyl)trifluorophosphate. In the oxidized form, every third to fourth benzene unit in the polymer carried a positive charge. This charge was compensated by the incorporation of anions from the ionic liquid. The mass increase was larger than expected from the electrochemically determined degree of doping, which is why the incorporation of additional ionic liquid in the polymer film had to be assumed. As the anion of the ionic liquid was very large, the preservation of electroneutrality during repeated reduction and oxidation of the polymer in benzene-free ionic liquid included a significant amount of cation exchange, especially at high scan rates. The polymer showed a porous, rough morphology with threadlike polymer strands.

Acknowledgment. Part of this work was funded by the Deutsche Forschungsgemeinschaft. A.B. would like to thank the Fonds der Chemischen Industrie for financial support. Merck KGaA is gratefully acknowledged for some free samples of [HMIm]FAP.

Appendix

In this paper, eq 9 was used in order to calculate potential-dependent anion exchange coefficients. However, eq 9 does not take electroless expulsion of ionic liquid, which is the equivalent to salt expulsion in the literature, into account. The following discussion is performed for the reduction of the polymer. All formulas are valid for the oxidation reaction as well.

The total number of moles of electrons injected into the polymer during reduction must be equal to the sum of cations inserted into the polymer and anions removed from the polymer

$$\frac{\mathrm{d}n_e}{\mathrm{d}t} = \frac{\mathrm{d}n_c}{\mathrm{d}t} - \frac{\mathrm{d}n_a}{\mathrm{d}t} = z_c \cdot \frac{\mathrm{d}n_e}{\mathrm{d}t} + z_a \frac{\mathrm{d}n_e}{\mathrm{d}t}$$

$$i = \frac{\mathrm{d}Q}{\mathrm{d}t} = -F \cdot \frac{\mathrm{d}n_e}{\mathrm{d}t} = -F \cdot \frac{\mathrm{d}n_c}{\mathrm{d}t} + F \cdot \frac{\mathrm{d}n_a}{\mathrm{d}t} \qquad (12)$$

dn_e: electrons injected into (dn_e > 0, reduction) or removed from (dn_e < 0, oxidation) polymer dn_a: anions exchanged for charge neutrality ($\leq$0 during reduction and expulsion; $\geq$0 during oxidation and insertion) dn_c: cations exchanged for charge neutrality ($\geq$0 during reduction and insertion; $\leq$0 during oxidation and expulsion)

The mass change of the polymer can be calculated from the changes in the amounts of anions and cations needed to maintain charge neutrality (and thus directly related to the current) and the amount of additional ionic liquid, which is transferred without current

$$\frac{\mathrm{d}m}{\mathrm{d}t} = \frac{\mathrm{d}n_c}{\mathrm{d}t} \cdot M_c + \frac{\mathrm{d}n_a}{\mathrm{d}t} \cdot M_a + \frac{\mathrm{d}n_{IL}}{\mathrm{d}t} \cdot (M_a + M_c) \qquad (13)$$

dn_{IL}: electroless change in the amount of ionic liquid in the film M_a, M_c, M_{IL}: Molar masses of IL anion and IL cation and the sum of both.

The differential mass−charge ratio can be calculated by dividing eqs 13 and 12

$$\frac{\mathrm{d}m}{\mathrm{d}Q} = \frac{\frac{\mathrm{d}n_c}{\mathrm{d}t} \cdot M_c + \frac{\mathrm{d}n_a}{\mathrm{d}t} \cdot M_a + \frac{\mathrm{d}n_{IL}}{\mathrm{d}t} \cdot M_{IL}}{-F \cdot \frac{\mathrm{d}n_e}{\mathrm{d}t}}$$

$$= \frac{(1 - z_a) \cdot \frac{\mathrm{d}n_e}{\mathrm{d}t} \cdot M_c - z_a \cdot \frac{\mathrm{d}n_e}{\mathrm{d}t} \cdot M_a + \frac{\mathrm{d}n_{IL}}{\mathrm{d}t} \cdot M_{IL}}{-F \cdot \frac{\mathrm{d}n_e}{\mathrm{d}t}} \qquad (14)$$

Equation 14 can be rearranged using eq 12

$$-F \cdot \frac{\mathrm{d}m}{\mathrm{d}Q} = M_c - \left[z_a + F \cdot \left(\frac{\mathrm{d}n_{IL}}{I\,\mathrm{d}t} \right) \right] \cdot M_{IL}$$

$$[z_a]_{app} = z_a + F \cdot \left(\frac{\mathrm{d}n_{IL}}{I\,\mathrm{d}t} \right) = \frac{M_c + F\left(\frac{\mathrm{d}m}{\mathrm{d}Q} \right)}{M_{IL}} \qquad (15)$$

The form of eq 15 is identical to that of eq 9, except that an apparent exchange coefficient is obtained including the contribution from the ionic liquid. The equation confirms that the expulsion of ionic liquid from the polymer (dn_{IL} < 0) during reduction (I < 0) indeed will cause the apparent anion exchange coefficients to be larger than the true values. For dn_{IL} = 0, eq 9 is obtained.

The same procedure can be applied to derive the apparent cation exchange coefficient. From the results, one obtains immediately

$$[z_a]_{app} + [z_c]_{app} = 1 \qquad (16)$$

Indifferent to real exchange coefficients, the apparent coefficients can become larger than 1, as well as negative.

References and Notes

(1) Shirakawa, H.; Louis, E.; MacDiarmid, A. G.; Chiang, C. K.; Heeger, A. J. *J. Chem. Soc., Chem. Commun.* **1977**, 578.
(2) Skotheim, T. A.; Elsenbaumer, R. L.; Reynolds, J. R. *Handbook of conducting polymers*, 2nd ed.; Marcel Dekker: New York, 1997.
(3) Jagur-Grodzinski, J. *Polym. Adv. Technol.* **2002**, *13*, 615.
(4) Grem, G.; Leditzky, G.; Ullrich, B.; Leising, G. *Adv. Mater.* **1992**, *4*, 36.
(5) Grem, G.; Leditzky, G.; Ullrich, B.; Leising, G. *Synth. Met.* **1992**, *51*, 383.
(6) Leising, G. *Phys. Bl.* **1993**, *49*, 510.
(7) Schindler, F.; Lupton, J. M.; Feldmann, J.; Scherf, U. *Proc. Natl. Acad. Sci. U.S.A.* **2004**, *101*, 14695.
(8) Shepard, A. F.; Dannels, B. F. *J. Polym. Sci., Part A: Polym. Chem.* **1966**, *4*, 511.

(9) Aeiyach, S.; Soubiran, P.; Lacaze, P. C.; Froyer, G.; Pelous, Y. *Synth. Met.* **1995,** *68*, 213.
(10) Kvarnström, C.; Bilger, R.; Ivaska, A.; Heinze, J. *Electrochim. Acta* **1998**, *43*, 355.
(11) Lère-Porte, J. P.; Radi, M.; Chorro, C.; Petrissans, J.; Sauvajol, J. L.; Gonbeau, D.; Pfister-Guillouzo, G.; Louarn, G.; Lefrant, S. *Synth. Met.* **1993**, *59*, 141.
(12) Kobryanskii, V. M.; Arnautov, S. A. *Synth. Met.* **1993**, *55*−*57*, 1371.
(13) Goldenberg, L. M.; Osteryoung, R. A. *Synth. Met.* **1994**, *64*, 63.
(14) Arnautov, S. A. *Synth. Met.* **1997**, *84*, 295.
(15) Endres, F. *ChemPhysChem* **2002**, *3*, 144.
(16) Endres, F. *Z. Phys. Chem. (Muenchen)* **2004**, *218*, 255.
(17) Buzzeo, M. C.; Evans, R. G.; Compton, R. G. *ChemPhysChem* **2004**, *5*, 1107.
(18) Wasserscheid, P., Welton, T., Eds. *Ionic liquids in synthesis*, 1st ed.; Wiley−VCH: Weinheim, 2002.
(19) Zein El Abedin, S.; Borrissenko, N.; Endres, F. *Electrochem. Commun.* **2004**, *6*, 422.
(20) Buttry, D. A.; Ward, M. D. *Chem. Rev.* **1992**, *92*, 1355.
(21) Kipling, A. L.; Thompson, M. *Anal. Chem.* **1990**, *62*, 1514.
(22) Glidle, A.; Hillman, A. R.; Bruckenstein, S. *J. Electroanal. Chem.* **1991**, *318*, 411.
(23) Martin, S. J.; Granstaff, V. E.; Frye, G. C. *Anal. Chem.* **1991**, *63*, 2272.
(24) Schröder, J.; Borngräber, R.; Lucklum, R.; Hauptmann, P. *Rev. Sci. Instrum.* **2001**, *72*, 2750.
(25) Tabidze, A. A.; Kazakov, R. Kh. *Meas. Tech. (Engl. Transl.)* **1983**, *26*, 24.
(26) Johannsmann, D.; Mathauer, K.; Wegner, G.; Knoll, W. *Phys. Rev. B* **1992**, *46*, 7808.
(27) Sauerbrey, G. *Z. Phys.* **1959**, *155*, 206.
(28) Lucklum, R.; Behling, C.; Hauptmann, P. *Sens. Actuators, B* **2000**, *65*, 277.
(29) Bund, A.; Schneider, O.; Dehnke, V. *Phys. Chem. Chem. Phys.* **2002**, *4*, 3552.
(30) Bund, A.; Schneider, M. *J. Electrochem. Soc.* **2002**, *149*, E331.
(31) Reynolds, J. R.; Sundaresan, N. S.; Pomerantz, M.; Basak, S.; Baker, C. K. *J. Electroanal. Chem.* **1988**, *250*, 350.
(32) Naoi, K.; Lien, M.; Smyrl, W. H. *J. Electrochem. Soc.* **1991**, *138*, 440.
(33) Otero, T. F.; Rodriguez, J. *Electrochim. Acta* **1994**, *39*, 245.
(34) Bilger, R.; Heinze, J. *Synth. Met.* **1991**, *41*−*43*, 2893.
(35) Dusemund, C.; Schwitzgebel, G. *Ber. Bunsen-Ges. Phys. Chem.* **1991**, *95*, 1543.
(36) Hillman, A. R.; Swann, M. S.; Bruckenstein, S. *J. Phys. Chem.* **1991**, *95*, 1543.
(37) Dusemund, C.; Schwitzgebel, G. *Synth. Met.* **1993**, *55*−*57*, 1396.
(38) Bruckenstein, S.; Brzezinska, K.; Hillman, A. R. *Phys. Chem. Chem. Phys.* **2000**, *2*, 1221.
(39) Hillman, A. R.; Glidle, A. *Phys. Chem. Chem. Phys.* **2001**, *3*, 3447.
(40) Jureviciute, I.; Bruckenstein, S.; Hillman, A. R.; Jackson, A. *Phys. Chem. Chem. Phys.* **2000**, *2*, 4193.
(41) Suematsu, S.; Oura, Y.; Tsujimoto, H.; Kanno, H.; Naoi, K. *Electrochim. Acta* **2000**, *45*, 3813.
(42) Bund, A.; Baba, A.; Berg, S.; Johannsmann, D.; Lubben, J.; Wang, Z.; Knoll, W. *J. Phys. Chem. B* **2003**, *107*, 6743.
(43) Henderson, M. J.; French, H.; Hillman, A. R.; Vieil, E. *Electrochem. Solid State Lett.* **1999**, *2*, 631.
(44) Henderson, M. J.; Hillman, A. R.; Vieil, E. *Electrochim. Acta* **2000**, *45*, 3885.
(45) Barbero, C.; Calvo, E. J.; Etchenique, R.; Morales, G. M.; Otero, M.; *Electrochim. Acta* **2000**, *45*, 3895.
(46) Bund, A.; Schwitzgebel, G. *Electrochim. Acta* **2000**, *45*, 3703.
(47) Efimov, I.; Winkels, S.; Schultze, J. W. *J. Electroanal. Chem.* **2001**, *499*, 169.
(48) http://www.ionicliquids-merck.de (October, 2004).
(49) Kanazawa, K. K.; Gordon, J. G., II *Anal. Chim. Acta* **1985**, *75*, 99.
(50) Martin, S. J.; Frye, G. C.; Wessendorf, K. O. *Sens. Actuators* **1994**, *44*, 209.
(51) Bund, A.; Schwitzgebel, G. *Anal. Chem.* **1998**, *70*, 2584.
(52) Bilger, R.; Heinze, J. *Synth. Met.* **1993**, *55*−*57*, 1424.
(53) Bandey, H. L.; Gonsalves, M.; Hillman, A. R.; Glidle, A.; Bruckenstein, S. *J. Electroanal. Chem.* **1996**, *410*, 219.
(54) Behling, C. Ph.D. Thesis, Otto-von Guericke Universität Magdeburg, Germany, 1999**.**
(55) Salomäki, M.; Loikas, K.; Kankare, J. *Anal. Chem.* **2003**, *75*, 5895.
(56) Lucklum, R.; Behling, C.; Hauptmann, P.; Cernosek, R. W.; Martin, S. J. *Sens. Actuators, A* **1998**, *66*, 184.
(57) Skompska, M.; Jackson, A.; Hillman, A. R. *Phys. Chem. Chem. Phys.* **2000**, *2*, 4748.
(58) Etchenique, R. A.; Calvo, E. J. *Electrochem. Commun.* **1999**, *1*, 167.
(59) Hornsteiner, J.; Born, E.; Fischerauer, G.; Riha, E. *Proc. IEEE Int. Freq. Control Symp.* **1988**, 615.
(60) Etchenique, R.; Brudny, V. L. *Langmuir* **2000**, *16*, 5064.
(61) Daikhin, L.; Gileadi, E.; Katz, G.; Tsionsky, V.; Urbakh, M.; Zagidulin, D. *Anal. Chem.* **2002**, *74*, 554.
(62) Bandey, H. L.; Hillman, A. R.; Brown, M. J.; Martin, S. *Faraday Discuss.* **1997**, *107*, 105.
(63) Vogt, B. D.; Lin, E. K.; Wu, W.; White, C. C. *J. Phys. Chem. B* **2004**, *108*, 12685.